

# Well-localized edge states in two-dimensional topological insulators: ultrathin Bi films

M. Wada,<sup>1</sup> S. Murakami,<sup>1,2</sup> F. Freimuth,<sup>3</sup> and G. Bihlmayer<sup>3</sup>

<sup>1</sup>*Department of Physics, Tokyo Institute of Technology, Ookayama, Meguro-ku, Tokyo 152-8551, Japan*

<sup>2</sup>*PRESTO, Japan Science and Technology Agency (JST), Kawaguchi, Saitama 332-0012, Japan*

<sup>3</sup>*Institut für Festkörperforschung and Institute for Advanced Simulation, Forschungszentrum Jülich, D-52425 Jülich, Germany*  
(Dated: October 30, 2018)

We theoretically study the generic behavior of the penetration depth of the edge states in two-dimensional quantum spin Hall systems. We found that the momentum-space width of the edge-state dispersion scales with the inverse of the penetration depth. As an example of well-localized edge states, we take the Bi(111) ultrathin film. Its edge states are found to extend almost over the whole Brillouin zone. Correspondingly, the bismuth (111) 1-bilayer system is proposed to have well-localized edge states in contrast to the HgTe quantum well.

PACS numbers: 73.43.-f, 72.25.Dc, 73.20.At, 85.75.-d

*Introduction*– The quantum spin Hall (QSH) phase [1, 2] is a new state of matter predicted theoretically, and has received a lot of attention recently. This phase is a nonmagnetic insulator in the bulk or film, and has gapless surface or edge states. The edge states consist of counterpropagating states with opposite spins. The notable feature of these edge states is that they are topologically protected; they remain gapless even in the presence of nonmagnetic impurities and interaction [3, 4]. We still know few systems in which the QSH phase is realized. The first theoretical proposal for the QSH system on the Bi ultrathin film by one of the authors [5]. In addition, HgTe quantum well has been theoretically proposed [6], and experimentally shown to be in the 2D QSH state [7, 8].

The edge states are localized near the edge, but their penetration depth  $\ell$  into the bulk varies between the systems. The observation and control of the edge states crucially depends on the penetration depth, and it is an important issue how they are determined in various systems. In the present paper we study the behavior of penetration depth  $\ell$  in QSH systems. From a simple model we show that the minimum penetration depth (which is typically reached in the middle of the bulk gap) scales with the inverse of the extension of the edge states in  $k$ -space. Therefore, if the edge states exist only in a small region in  $k$ -space,  $\ell$  is long. By extending this conclusion to generic cases, we expect that the penetration depth is of the order of the lattice constant, if the edge state extends almost over the whole Brillouin zone. To see this, we numerically study topological properties of bismuth ultrathin films and their edge states. Among bismuth thin films, only two thin films are proposed to be insulating in the bulk: the (111) single (1) -bilayer film [9] and the {012} 2-monolayer film [10]. By using tight-binding Hamiltonians obtained by first-principles calculations, we found that (111) 1-bilayer film is in the QSH phase and {012} 2-monolayer film is not. We also found that the edge states in Bi (111) 1-bilayer film are well localized near the edges, compared with the HgTe quantum well. From these studies we conclude that the penetration depth  $\ell$  corresponds to the inverse of the  $k$ -space width of edge-state dispersion.

*Penetration depth of the edge states*– We use the Hamilto-

nian for the HgTe quantum well.

$$\mathcal{H}(k_x, k_y) = \begin{pmatrix} H(\mathbf{k}) & 0 \\ 0 & H^*(-\mathbf{k}) \end{pmatrix}, \quad (1)$$

where  $H(\mathbf{k}) = \epsilon_{\mathbf{k}} \mathbf{I}_2 + d^a(\mathbf{k}) \sigma^a$ . Here,  $\mathbf{I}_2$  is a  $2 \times 2$  unit matrix,  $\sigma_a$  the Pauli matrices,  $\epsilon_{\mathbf{k}} = C - D(k_x^2 + k_y^2)$ ,  $d^1 = Ak_x$ ,  $d^2 = Ak_y$ , and  $d^3 = \mathcal{M}(k) = M - B(k_x^2 + k_y^2)$ . The constant  $C$  is set to zero since it is an overall energy offset. The eigenenergies are then given by  $-Dk^2 \pm |\mathbf{d}(\mathbf{k})|$ . Thus  $D$  represents the asymmetry between the valence and the conduction band dispersions. The bulk gap at  $\mathbf{k} = 0$  is given by  $2M$ . In order to consider the edge state on a single edge, we deal with a system on a half-plane of  $y \leq 0$ . This considerably simplifies the results, compared with the ribbon of finite width [11]. As edge states only the solutions with  $e^{\lambda y}$  ( $\text{Re}\lambda > 0$ ) are allowed. The secular equation

$$(M - E + B_+(\lambda^2 - k_x^2))(-M - E - B_-(\lambda^2 - k_x^2)) = A^2(k_x^2 - \lambda^2), \quad (2)$$

where  $B_{\pm} = B \pm D$ , gives two allowed values for  $\lambda$ :

$$\lambda = \lambda_{1,2} = \sqrt{k_x^2 + F \pm \sqrt{F^2 - (M^2 - E^2)/(B_+ B_-)}}, \quad (3)$$

where  $F = \frac{A^2 - 2(MB + ED)}{2B_+ B_-}$ . If we impose a boundary condition  $\psi(y=0) = 0$  as in [11], we get

$$\lambda_1 \lambda_2 = \frac{BM + DE}{B_+ B_-} - k_x^2, \quad \lambda_1 + \lambda_2 = \frac{DM + BE}{k_x B_+ B_-}. \quad (4)$$

From Eqs. (3) and (4), we obtain an exact form for the dispersion of edge states

$$E = -\frac{DM}{B} \pm \frac{A}{B} \sqrt{B_+ B_-} k_x. \quad (5)$$

The signs correspond to the two branches of edge states with opposite spins. Because they are related with each other by Kramers theorem, we henceforth consider only the plus sign in (5). Putting (5) into (4), we get

$$\lambda_1 \lambda_2 = -k_x^2 + \frac{2DN}{B} k_x + \frac{M}{B}, \quad \lambda_1 + \lambda_2 = 2N, \quad (6)$$

where  $N = A/(2\sqrt{B_+B_-})$ . These determine  $\lambda_{1,2}$ . If we put  $\lambda_1 > \lambda_2$ ,  $\lambda_2^{-1}$  gives the physical penetration depth  $\ell$  as discussed in [11]. At the points with  $\lambda_2 = 0$ , the edge states have infinite penetration depth and become bulk states. From (6) this occurs when  $k_x = k_x^\pm \equiv \frac{DN}{B} \left(1 \pm \sqrt{1 + \frac{BM}{D^2N^2}}\right)$ . It can be checked that the states at  $k_x = k_x^\pm$  are located at the band edge of the projection of the bulk band, and at these points the edge dispersion (5) is tangential to the bulk band projection. We can rewrite as  $\lambda_1\lambda_2 = -(k_x - k_x^+)(k_x - k_x^-)$ . Therefore  $\lambda_2 (= \ell^{-1})$  is expressed as  $\ell^{-1} = N - \sqrt{N^2 + (k_x - k_x^+)(k_x - k_x^-)}$ . Hence the behavior of  $\ell^{-1}$  is as shown in Fig. 1. It vanishes at the points  $P_\pm$  ( $k_x = k_x^\pm$ ) where the edge states are absorbed into the bulk band, and  $\ell$  is minimum when  $k_x = (k_x^+ + k_x^-)/2$ . The minimum value  $\ell_{\min}$  is given by  $\ell_{\min}^{-1} = N - \sqrt{N^2 - (k_x^+ - k_x^-)^2/4}$ . As a function of  $N$ , the minimum value of  $\ell_{\min}$  is  $2/(k_x^+ - k_x^-)$  at  $N = (k_x^+ - k_x^-)/2$ . This means that the minimum  $\ell_{\min}$  of the system is roughly given by the inverse of the  $k$ -space extension of the edge state dispersion. From Fig. 1 it can be seen that the penetration depth  $\ell$  becomes short when the considered edge state is far from the points  $P_\pm$ . The inverse of the penetration depth  $\ell^{-1}$  corresponds to an imaginary part of the wavenumber perpendicular to the edge direction, and therefore it behaves similarly to the (real) wavenumber. Hence  $\ell^{-1}$  is approximately given by the  $k$ -space distance of wavenumbers from the points  $P_\pm$ .

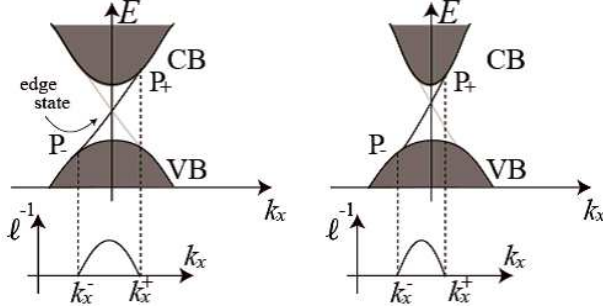


FIG. 1: Penetration depth  $\ell$  for the effective model with ribbon geometry. CB (VB) represents the bulk conduction (valence) band. The plot on the right corresponds to a more asymmetric situation, leading to a larger  $\ell$  at the crossing point of the edge states.

In the HgTe quantum wells, the 2D quantum spin Hall states are confirmed by transport measurements [7, 8]. The penetration depth of the edge states in these systems has been calculated to be relatively long  $\ell \sim 50\text{nm}$  [11]. In our theory, by plugging the parameters into our results, we get  $\ell = 56\text{nm}$  at  $k_x = 0$ , in agreement with [11]. The coefficient  $D$  gives rise to an asymmetry between the conduction and the valence bands, and the edge state is also asymmetric:  $k_x^+ \neq -k_x^-$ ,  $k_x^+ = 0.62\text{nm}^{-1}$ ,  $k_x^- = -0.024\text{nm}^{-1}$ . Thus the penetration depth  $\ell$  is shortest not at  $k_x = 0$  but at  $k_x = (k_x^+ + k_x^-)/2 = 0.30\text{nm}^{-1}$  with  $\ell_{\min} \sim 6.2\text{nm}$ . In our interpretation, the relatively long  $\ell$  of the edge states in

HgTe quantum well comes from the fact that the edge states are localized within a very narrow region in  $k$  space, giving a long  $\ell$ . This penetration depth determines the minimal width of the system size required for observation of edge states.

*Bi(111) Ultrathin Film*— By extending our theory to generic types of edge states, we can expect that the inverse of the penetration depth  $\ell^{-1}$  well scales with the  $k$ -space distance from the absorption point  $P_\pm$  into the bulk band. Therefore, if the edge states extend over the Brillouin zone, the penetration depth of the edge states is as short as a few lattice constants. We will theoretically show that Bi(111) ultrathin film is a QSH system having edge states with such a short penetration depth.

For the calculation, we use a tight-binding model constructed from maximally localized Wannier orbitals [12] obtained from first-principle calculations [13]. The Fermi energy lies in the 6p-like states, comprising three conduction bands and three valence bands. Therefore, in constructing the Wannier orbitals we only retain these six bands. From these Wannier orbitals including the lattice relaxation effects of the ultrathin films, we construct tight-binding models keeping up to third-neighbor hopping amplitudes.

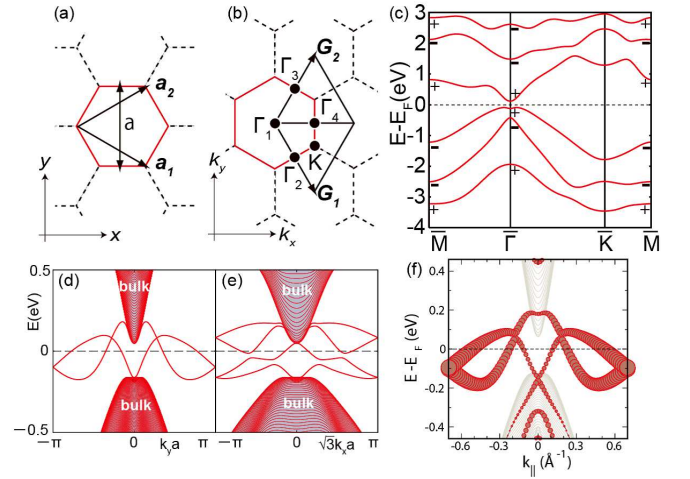


FIG. 2: (a) Unit cell and lattice vectors, and (b) TRIMs of Bi(111) ultrathin film. The TRIM  $\Gamma_1$  is the  $\Gamma$  point, and the three TRIMs  $\Gamma_2, \Gamma_3$  and  $\Gamma_4$  are the  $M$  points. (c) Bulk energy bands and the parity at the TRIMs for a Bi(111) 1-bilayer. (d) and (e): Energy bands of the Bi(111) zigzag and armchair edge ribbons, respectively, with a width of 20 unit cells, calculated from tight-binding model. (f) Energy bands of a eight-unit-cell wide Bi(111) zigzag edge ribbon from first-principles calculations. The size of the symbols corresponds to the weight of the states in the edge atoms.

Figures 2 (a – c) show the unit cell and lattice vectors, reciprocal vectors and TRIMs, and the energy band of Bi(111) 1-bilayer respectively. Since this system is inversion symmetric, all states in Fig. 2 (c) are doubly degenerate. This system is proposed to be a nonmagnetic insulator with a bulk gap of  $\sim 0.2\text{eV}$  [9]. We will calculate the  $Z_2$  topological number  $\nu$ , and if it is nontrivial it is a QSH insulator. The wavenumbers satisfying  $\mathbf{k} \equiv -\mathbf{k} \pmod{\mathbf{G}}$  are called time-

reversal-invariant momenta (TRIM)  $\mathbf{k} = \Gamma_i$  ( $i = 1, 2, 3, 4$ ). For inversion-symmetric systems, the  $Z_2$  topological number  $\nu$  is defined by  $(-1)^\nu \equiv \prod_{i=1}^4 \prod_{m=1}^n \xi_{2m}(\Gamma_i)$  ( $= \pm 1$ ), where  $\xi_{2m}(\Gamma_i)$  ( $= \pm 1$ ) is the parity eigenvalue of the Kramers pairs at  $\Gamma_i$  and  $n$  is the number of the Kramers pairs of eigenstates below the Fermi energy [14]. The parity eigenvalues at the TRIMs  $\Gamma_i$  ( $i = 1, 2, 3, 4$ ) are given in Fig. 2 (c) and yield the topological number  $\nu = 1$ . We note that both the first-principle calculation (without a tight-binding model) and the calculation of the Liu-Allen tight-binding model [15] give  $\nu = 1$ . In Ref. [5] a (111) 1-bilayer bismuth is proposed to be in the QSH phase, from a simple truncation of the 3D tight-binding model [15]. We thus confirmed that the conclusion in Ref. [5] remains unaltered in first-principle calculations.

If we neglect the out-of-plane coordinate, the (111) 1-bilayer film has a honeycomb structure. Therefore, as in graphene we refer to the two types of simple edge shapes as zigzag and armchair edges. Figure 2 (d)(e) shows the energy bands of zigzag and armchair edge ribbons of the Bi(111) 1-bilayer. Due to inversion symmetry, all the states are doubly degenerate, and they have opposite spins, localized on the opposite edges. In both figures, the number of Kramers pairs of edge states on the Fermi energy per one edge is odd, confirming that Bi(111) 1-bilayer is a QSH system. We checked that for the zigzag-edge ribbon our result from the tight-binding model (Fig. 2 (d)) and that from a first-principle calculation (Fig. 2 (f)) are in good agreement.

These edge states are quite different from those in a HgTe quantum well, where the edge states exist only near the  $k = 0$  point [6]. Within our calculation, the edge states extend almost all over the whole Brillouin zone. At the Fermi energy there are three Kramers pairs of edge states. Thus, the conductance in a ribbon geometry becomes  $G = 6e^2/h$  for a clean system. When nonmagnetic disorder is increased, some of these edge states become gapped due to elastic scattering, while at least one pair of edge states remain gapless, giving the conductance of  $G = 2e^2/h$ . These edge states form perfectly conducting channels, similar to those in the graphene nanoribbons [16]. In graphene, perfectly conducting channels are formed only in the absence of short-ranged disorder; in the Bi (111) 1-bilayer nanoribbon the perfectly conducting channel exists irrespective of the nature of nonmagnetic disorder, and it gives a universal behavior realizable in experiments.

*Bi{012} ultrathin film*– For inversion asymmetric systems such as Bi {012} 2-monolayer film, the calculation of  $\nu$  is complicated because the phases of the Bloch wavefunctions in the entire Brillouin zone are involved [1, 17]. The phase of the wavefunction is a gauge degree of freedom and can be chosen arbitrary for each  $\mathbf{k}$ . Hence, a simple discretization of a formula for continuous  $\mathbf{k}$  suffers from numerical instability due to this gauge choice.

Hence, we adopt a gauge-invariant discretization method proposed in Ref. [18]. It is a merit of the method that we do not need to determine the phase of the wavefunction smoothly in  $\mathbf{k}$  space. The mesh size  $\delta k_1 \delta k_2$  should be fine enough to satisfy  $|F(\mathbf{k})| \delta k_1 \delta k_2 < \pi$  at any mesh, where  $F(\mathbf{k})$  is the

Berry curvature, and  $\delta k_1, \delta k_2$  are the width and height of a mesh, respectively [18]. This quantity is largest when  $\mathbf{k}$  is at the direct gap  $\mathbf{k} = \mathbf{k}_g$ , and the critical size is approximated by the  $\mathbf{k}$ -space nominal size of the band extremum at  $\mathbf{k} = \mathbf{k}_g$ . From the band structure of Bi{012} 2-monolayer, the critical mesh number  $n_B^c$  is estimated to be  $\sim 100$ . For various mesh numbers exceeding  $n_B^c$  we get the consistent result that the  $Z_2$  topological number is  $\nu = 0$ . Therefore, Bi{012} 2-monolayer is an ordinary insulator.

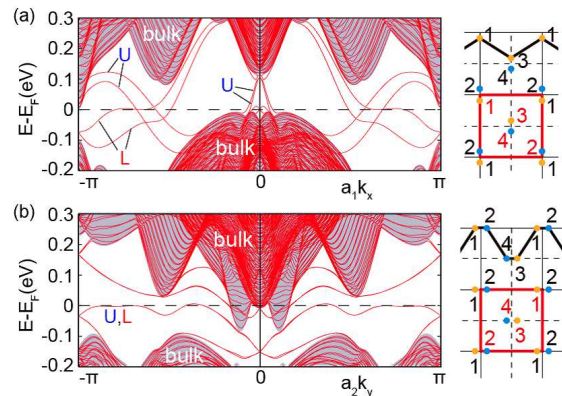


FIG. 3: Energy bands of Bi{012}: (a) zigzag and (b) armchair edge ribbons with a width of 20 unit cells. ‘U’ (‘L’) means that the state is localized on the upper (lower) edge. The crystal structures near the upper edge are shown in the right panels with 1,2,3 and 4 representing the lattice sites. We note that these 4 sites do not lie on the same plane. The shaded regions are the bulk energy bands.

The edge states for ribbons with two types of edges of Bi{012} 2-monolayer ribbons and their energy bands are shown in Fig. 3. The two edge shapes can be called zigzag and armchair edges, although the lattice structure is quite different from graphene. The number of Kramers pairs of edge states on the Fermi energy is even at each edge and this is in agreement with our result that the  $Z_2$  topological number is  $\nu = 0$ . In the armchair-edge ribbon, the edge states are almost degenerate because of the equivalence of two edges of the ribbon via mirror-symmetry. These two states have an energy difference, due to hybridization of the edge states at the opposite edges. Nevertheless, for a ribbon wider than  $\ell$ , the energy difference is exponentially small. On the contrary, in the zigzag-edge ribbon, the edge states are not degenerate because of inequivalence between both edges of the ribbon.

*Penetration depth of the edge states*– We now calculate the penetration depth  $\ell$  of the edge states of the Bi(111) 1-bilayer film. For the edge states on the zigzag edge of the (111) 1-bilayer film, the result is shown in Fig. 4 (i). The penetration depths  $\ell$  of the edge states (including those on the Fermi energy) are typically several lattice constants. Hence, for transport experiments the width of the sample has to be larger than a few lattice constants.

These results on Bi(111) film agree with our theory on  $\ell$ . According to our theory, the penetration depth  $\ell$  becomes short when the edge states are distant from the points

$P_{\pm}$  where the edge states merge into the bulk (circles in Fig. 4(ii)(iii)). Hence,  $\ell$  is longer for the states at  $E_F$  in Fig. 4 (ii), and shorter in Fig. 4 (iii). This information is relevant for transport which is governed by the states at the Fermi level. In Bi(111), the edge state travels almost over the whole Brillouin zone (BZ). Therefore we estimate  $\ell \sim (\text{size of the BZ})^{-1} \sim$  (lattice spacing), in agreement with the results in Fig. 4(i)

Bi(111) 1-bilayer film cannot be described by an effective model near  $\mathbf{k} = 0$  like (1). The effective model (1) is derived when the QSH system is described as a band inversion between two doubly-degenerate bands, such as HgTe quantum well, or  $\text{Bi}_2\text{Se}_3$ . In bismuth ultrathin films, the involved bands are  $p_x, p_y, p_z$  orbitals, and the valence and conduction bands have different mixing coefficients for these orbitals. Therefore, it is not a mere band inversion, which is the reason why the case Fig. 4(iii) is realized in bismuth films.  $\text{Bi}_2\text{Te}_3$  and  $\text{Bi}_2\text{Se}_3$  ultrathin films also have edge states similar to Fig. 4(iii) [19]. In these cases, however, some edge states are close to the bulk bands, leading to very long penetration depths of about a hundred times the lattice constant. We note that our theory assumes isotropy between the direction along the edge/surface and that perpendicular to it. For layered materials such as  $\text{Bi}_2\text{Se}_3$  and  $\text{Bi}_2\text{Te}_3$ , the penetration depth perpendicular to the layer cannot be predicted from the surface-state dispersion in the layer because of the anisotropy.

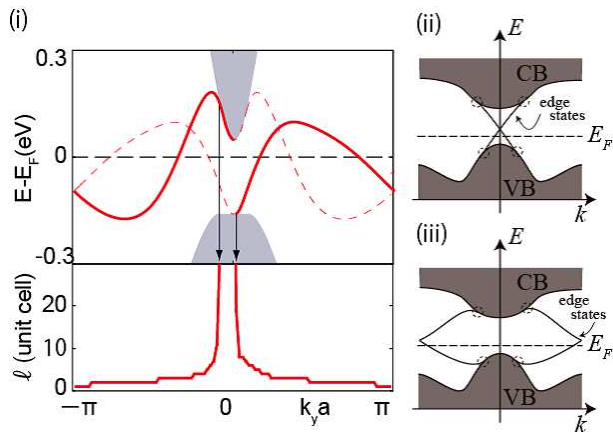


FIG. 4: (i) Penetration depth of the edge states on the zigzag edge of the Bi(111). (ii)(iii) Examples of the edge states in the 2D QSH systems.

These short penetration depths of edge states in the Bi (111) 1-bilayer film are ideal for observation by STM/STS and control of the edge states. Furthermore, it is also favorable for

edge thermoelectric transport [20]. To utilize the perfectly conducting channels of edge states for thermoelectric transport, short penetration depth is an important factor, because longer penetration depth mixes the states at different edges for narrow ribbons, and destroys the coherent electron transport at the edges.

*Conclusion*– We analyze a generic behavior of the penetration depth of the edge states in two-dimensional quantum spin Hall systems. We found that momentum-space distance between the edge states and the absorption point of the edge dispersion into the bulk band roughly gives the inverse of the penetration depth. As an example, we calculate the penetration depth of the edge states of Bi(111) 1-bilayer film, which we propose to be a QSH insulator. The penetration depth of the edge states in Bi(111) 1-bilayer film is in good agreement with our theory.

We are grateful to S. Blügel, T. Hirahara, T. Nagao, and S. Yaginuma for helpful discussions. This research is supported in part by MEXT KAKENHI.

- 
- [1] C. L. Kane and E. J. Mele, Phys. Rev. Lett. **95**, 226801 (2005); *ibid.* **95**, 146802 (2005).
  - [2] B. A. Bernevig and S.-C. Zhang, Phys. Rev. Lett. **96**, 106802 (2006).
  - [3] C. Wu, B. A. Bernevig and S.-C. Zhang, Phys. Rev. Lett. **96**, 106401 (2006).
  - [4] C. Xu and J. E. Moore, Phys. Rev. B **73**, 045322 (2006).
  - [5] S. Murakami, Phys. Rev. Lett. **97**, 236805 (2006).
  - [6] B. A. Bernevig, T. L. Hughes and S.-C. Zhang, Science **314**, 1757 (2006).
  - [7] M. König *et al.*, Science **318**, 766 (2007).
  - [8] A. Roth, *et al.*, Science **325**, 294 (2009).
  - [9] Yu. M. Koroteev, G. Bihlmayer, E. V. Chulkov, and S. Blügel, Phys. Rev. B **77**, 045428 (2008).
  - [10] S. Yaginuma, *et al.*, J. Phys. Soc. Jpn. **77**, 014701 (2008).
  - [11] B. Zhou *et al.*, Phys. Rev. Lett. **101**, 246807 (2008).
  - [12] N. Marzari and D. Vanderbilt, Phys. Rev. B **56**, 12847 (1997).
  - [13] F. Freimuth *et al.*, Phys. Rev. B **78**, 035120 (2008).
  - [14] L. Fu and C. L. Kane, Phys. Rev. B **76**, 045302 (2007).
  - [15] Y. Liu and R. E. Allen, Phys. Rev. B **52**, 1566 (1995).
  - [16] K. Wakabayashi, Y. Takane, and M. Sigrist, Phys. Rev. Lett. **99**, 036601 (2007).
  - [17] L. Fu and C. L. Kane, Phys. Rev. B **74**, 195312 (2006).
  - [18] T. Fukui and Y. Hatsugai, Phys. Soc. Jpn. **76**, 053702 (2007).
  - [19] C.-X. Liu *et al.*, Phys. Rev. B **81**, 041307(R) (2010).
  - [20] R. Takahashi and S. Murakami, Phys. Rev. B **81**, 161302(R) (2010).